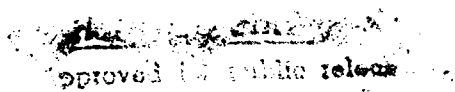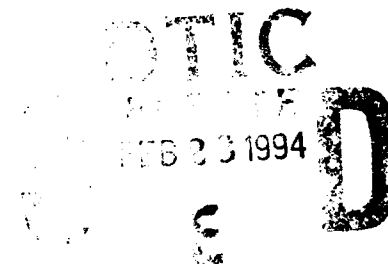AD-A276 217

PEAK DETECTION OF SWERLING TYPE TARGETS PART I: DETECTION PROBABILITIES IN WHITE NOISE

by

Anastasios Drosopoulos and George Haslam

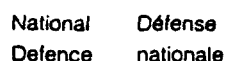# DEFENCE RESEARCH ESTABLISHMENT OTTAWA
REPORT NO. 1193

94-06298

December 1993
Ottawa

94 2 25 008

I✦I National Défense
Defence nationale

PEAK DETECTION OF SWERLING TYPE TARGETS
PART I:
DETECTION PROBABILITIES IN WHITE NOISE

by

Anastasios Drosopoulos and George Haslam

Airborne Radar Section
Radar Division

DEFENCE RESEARCH ESTABLISHMENT OTTAWA
REPORT NO. 1193

Abstract

Peak detection is an alternative to the commonly used threshold detection scheme in radar systems. The present report is the first part in an investigation of peak detection performance, for Swerling type targets, in an arbitrarv noise/clutter background. In this report, peak detection is compared with classic fixed threshold detection in uncorrelated white noise. A methodology is also developed, capable of handling arbitrary stochastic signal and noise/clutter models.

Résumé

La méthode de détection par pic est une alternative possible à la technique de détection par seuillage, qui est largement utilisée dans les systèmes radars. Ce rapport discute d'une première étape d'une étude de performance de la méthode de détection par pic, pour des cibles du type Swerling, en présence de bruit et de fouilli arbitraires. Dans ce document, la détection par pic est comparée à la détection classique, par seuillage fixe, en présence de bruit blanc non-correllé. Une méthode capable de traiter les cas de signaux stochastiques arbitraires et de modèles arbitraires de bruit et de fouilli est aussi développée.

Executive Summary

Peak detection is an alternative to the commonly used threshold detection in radar systems. Classic, fixed threshold detection, compares the received signal samples with a threshold, derived from some probability model and a specified probability of false alarm, and estimates the probability of signal detection as a function of signal-to-noise-ratio. Peak detection, on the other hand, does not specifically employ a threshold. Instead, the signal maximum during a specified processing interval is taken as the desired output. This output follows the original signal variations more closely and the system gain for a specified probability of false alarm is much easier to set and presumably more robust.

     The present report carries out the first part of an investigation of peak detection performance in a typical radar system. This is done as follows:

1. The proper methodology is determined. The Monte-Carlo method with importance sampling is used here; the parameters of a given probability model are suitably scaled and the output weighted so that the "rare" events are seen more often. This results in considerable savings of simulation run-time.

2. The ideal peak detection performance is compared with ideal threshold detection performance, by computing probability of detection curves for all Swerling type targets in a white noise background. A comparison between fixed threshold detection and peak detection is performed in the classical way, by estimating a new threshold based on the modified probability model (the new probability density is the maximum order statistic of the unmodified density) for the same probability of false alarm. Results show that the drop from ideal performance, where one takes into account all incoming samples, to peak detection performance, where the maximum (peak) of a number of consecutive samples is taken, was of the order of a few dB for a 50 % or more probability of detection.

     The second part of the investigation, in a future report, will complete the peak detection performance evaluation, in a white noise background, by assuming a typical radar system, e.g. one suitable for periscope detection [8]. The effects of bandwidth reduction and collapsing losses will be examined and the overall detection performance established.

Finally, the third part will extend the noise/clutter background to cover K-distributed clutter. This is the commonly accepted model for sea clutter statistics. Noise/clutter correlation aspects will be covered, together with the design of the proper prewhitening filters.

Contents

List of Tables

List of Figures

1

Introduction

The radar detection process is normally carried out by comparing the received radar signal with a threshold value. This is the so-called threshold detection scheme. The threshold is determined from the assumed probability model of the noise/clutter background in which the signal propagates and a desired level of false alarm. In classic fixed threshold detection, this procedure is optimum for maximizing the probability of detection, provided that the assumed probability model for the noise/clutter background is correct.

As normally implemented, a biased diode establishes a threshold voltage level. The receiver gain for the incoming signal can then be adjusted, either manually or automatically, through some constant false alarm rate (CFAR) scheme. The combined effect is, that the signal is thresholded at a specific false alarm value. It turns out that the threshold value is extremely sensitive to the gain setting. A slight manual adjustment by the human operator, to make target discrimination on the video display easier, may easily affect adversely the desired probability of false alarm, P_{FA}, since the transition from a "dark" screen to one "flooded" with "targets" can be quite abrupt. A different detection process, with a smoother transition, would therefore be very useful in practical applications. Peak detection is a possible candidate for this task. Instead of comparing the incoming received signal samples (a digital approach is assumed) with a threshold, a number of consecutive samples are peak detected, i.e. the maximum sample value is retained for the sample duration.

Implementation of threshold detection leads to "0" and "1" pulses depending on the detector decision between "noise" and "signal". The "1" pulses are of equal intensity in this scheme. Peak detection introduces a "gray" scale to the detection process since the intensity variation of the incoming signal is followed more closely. Taking the peak value of several consecutive samples, in place of the samples themselves, considerably reduces the received signal bandwidth. Normally, there is some bandwidth reduction process, with effects similar to peak detection, inherent in a normal implementation of a radar receiver, either at the front end or on the video display. Such implementations lead to significant hardware simplifications that far outweigh the slight loss in detection

1

introduced by bandwidth reduction. For a thorough evaluation of overall detection performance, the effect of deliberately introducing the peak detection scheme at the front end of the receiver has to be quantitatively investigated and compared with the normal implementation.

In this report, the goal is to begin the investigation of peak detection performance by comparing it to classic fixed threshold detection. A non-correlated white noise background is assumed. The discussion of K-distributed clutter, which is more realistic for targets on the sea surface, and the prewhitening filters that should be used for the case of correlated clutter, are left to future reports. The proper methodology is also developed to handle arbitrary stochastic signal and noise/clutter models in preparation for that future work.

At this stage, it is not expected that the use of peak detection will exceed the performance obtained with optimum threshold detection. In fact, the loss is expected to be of the order of a few dB. However, the overall detection performance also depends on the specific bandwidth reduction scheme used and on the collapsing losses at the display unit. These losses are also of the order of a few dB. Part II of this investigation will address these issues, taking a specific radar system into consideration.

As already explained, the detector output signal is different for peak and fixed threshold detection. An approach has to be found for comparing the outputs in a meaningful way for the same P_{FA}. Fig. 1.1 illustrates the approach taken here.

The top left graph is a qualitative example of a typical received signal which includes signal and noise components. This is thresholded for a desired P_{FA}, taking into account a knowledge of the Probability Distribution Function, PDF, of the noise component. The output of this fixed threshold detection scheme is shown in the top right graph. The peak detector output is shown in the bottom left graph (solid rectangular curve). It is different from the fixed threshold detector output, and follows variations of the original input signal more closely. In order to compare the two cases, the peak detector output is thresholded as well, using the same P_{FA}. Note that the underlying PDF is different now. The thresholded peak detector output is shown in the bottom right graph. The two methods, top and bottom right graphs, can then be compared as follows. Noting that the time scale (x-axis) is the same for both graphs, the area under the pulses, divided by the the area within the entire observation interval, can be used to give the proportion of the signal present. This proportion, which is the probability of detection, P_D, can be graphed as a function of the signal-to-noise ratio for both cases.

The investigation begins with an outline of the known case of classic fixed threshold detection in a white noise background. The search for the proper methodology starts here, with a comparison and verification of the results with the known performance curves published in the literature [1]. The criteria for comparison are:

- ease of implementation,

- estimator accuracy, and
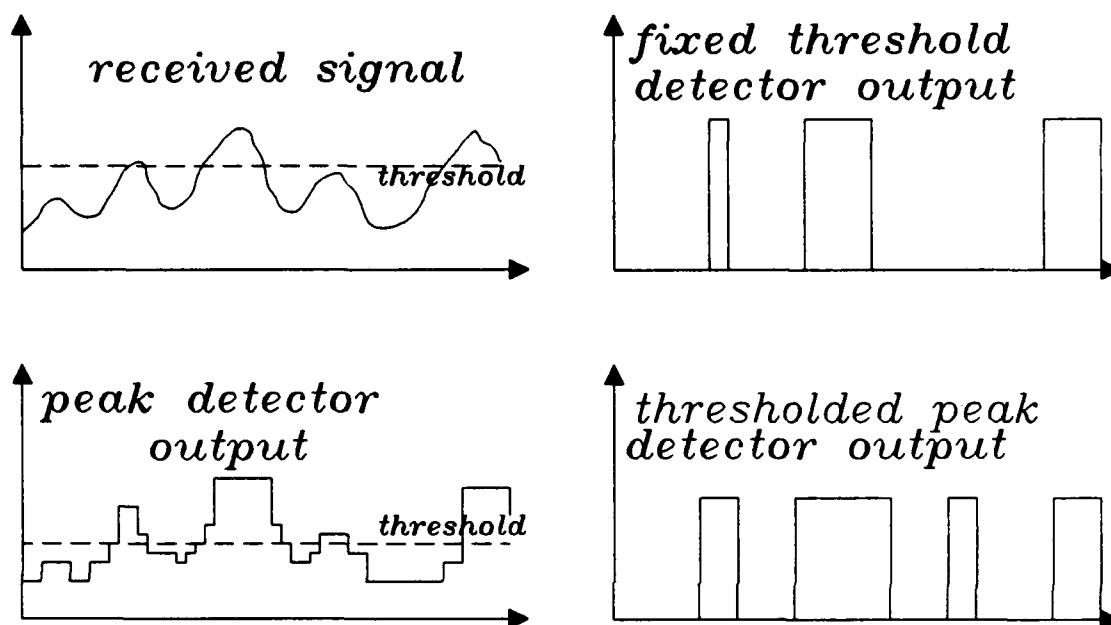
Figure 1.1: Scheme for comparing peak and fixed threshold detection.

4

- capability to handle arbitrary signal and noise structures.

The methodology finally chosen is that of Monte Carlo with importance sampling. The investigation then proceeds by computing peak detection performance curves, similar to those computed for fixed threshold detection, in an uncorrelated white noise background. The report concludes with a summary of the above results and outlines the work still required to complete a thorough investigation of overall peak detection performance.

2

Classic fixed threshold detection in white noise

The backscattered microwave signal, that arrives at the receiver from a target, in the presence of clutter and receiver noise, is assumed to be a train of N pulses. The five Swerling cases interpret this as follows:

Swerling 0: The target cross-section is constant, leading to a non-fluctuating pulse amplitude, with a constant peak-to-peak signal-to-noise ratio, R. The variable on reception is the initial phase of each pulse, which is assumed to be uniformly and independently distributed in $[0, 2\pi]$.

Swerling I: The target orientation changes slowly compared to the pulse-train duration; this results in a nearly undistorted pulse train, so that a single random variable can characterize the overall train amplitude. However, the target cross-section change is sufficiently large from scan-to-scan, to result in scan-to-scan fluctuations of the train amplitude, which are described by a Rayleigh probability density function. In addition, the initial phase of each pulse is assumed to be uniformly and independently distributed as in Swerling 0.

Swerling II: The cross-section fluctuations are rapid enough, so that each pulse in the train is a statistically independent random variable from the same Rayleigh distribution. Again, the initial phase of each pulse is assumed to be uniformly and independently distributed as in Swerling 0.

Swerling III: This is the same as Swerling I, except that the pulse-train amplitude comes from the one-dominant-plus-Rayleigh distribution; this distribution assumes a single dominant strong scatterer, together with many weaker ones in the resolution cell of the radar.

Swerling IV: Swerling IV is similar to Swerling II, except that each pulse amplitude comes from the one-dominant-plus-Rayleigh distribution.

In all cases, the receiver structure that gives optimum performance in comparison with a fixed threshold is the square law detector[1]. The Neyman-Pearson detection test, appropriate to the case of binary detection with a constant false alarm, is

$$H_0 : \quad r_i = n_i$$
$$H_1 : \quad r_i = s_i + n_i$$

where the ith observation of the received signal, r_i, is composed of noise only, which is hypothesis H_0, or signal plus noise, which is hypothesis H_1. The choice of one of the above hypotheses leads to a comparison of the test statistic with a threshold. The probability of detection, P_D, is the probability that the test statistic exceeds the threshold when a signal is present, and the probability of false alarm, P_{FA}, is the probability that the test statistic exceeds the threshold when only noise is present.

The test statistic for square law detection is [1]

$$x = \sum_{i=1}^{N} \frac{1}{2} r_i^2 = \sum_{i=1}^{N} x_i \quad ,$$

where the PDF of the received signal amplitude, r_i, for a single observation of signal plus noise is

$$p(r_i; R) = \begin{cases} r_i \exp[-(r_i^2 + R)/2] I_0(r_i\sqrt{R}) & r_i \geq 0 \\ 0 & r_i < 0 \end{cases}$$

The function I_0 above, is the zero order, modified Bessel function of the first kind, while the variable R, is the peak-to-peak signal-to-noise ratio. The PDF of $x_i = r_i^2/2$ is

$$p(x_i; R) = \begin{cases} \exp[-(x_i + R/2)] I_0(\sqrt{2x_i R}) & x_i \geq 0 \\ 0 & x_i < 0 \end{cases}$$

These are all special cases of the noncentral χ^2 distribution [10]. Note that, for the noise-only case, $R = 0$ and $I_0(0) = 1$. For Swerling 0, R is a constant while for the other Swerling cases, R is a random variable with its own PDF. The overall PDF of the test statistic x is

$$p(x) = \int_{-\infty}^{\infty} p(x|R) p(R) dR \quad .$$

The classic approach of fixed threshold detection, due to Marcum and Swerling [3, 9], is as follows:

- The test statistic, x, for a given R, is a sum of N independent random variables with a known PDF, $p(x_i; R)$. The PDF of x, $p(x; R)$, is the N-fold convolution of the individual $p(x_i; R)$'s [5]. In the Fourier domain, the characteristic function of x is the product of the characteristic functions of the x_i's. Taking the inverse Fourier transform of the characteristic function of x, $p(x; R)$ is derived.

---

[1] Actually this is strictly true for small signal-to-noise ratios, whereas the linear detector is "theoretically" optimum for the other extreme. Practically speaking however, the performance of both detectors is shown to be almost the same for all signal-to-noise ratios.

- The false alarm threshold, T_{FA}, for a given probability of false alarm, P_{FA}, is computed from

$$P_{FA} = \int_{T_{FA}}^{\infty} p(x;0)dx = 1 - \int_{0}^{T_{FA}} p(x;0)dx \quad . \tag{2.1}$$

- The probability of detection for a given R and P_{FA} is computed from

$$P_D = \int_{T_{FA}}^{\infty} p(x;R)dx = 1 - \int_{0}^{T_{FA}} p(x;R)dx \quad . \tag{2.2}$$

While straightforward in principle, the analytical approach leads to complicated integrals and special functions that require a variety of approximations before the final results can be derived with some degree of accuracy. A recent paper by Hou et al. [2] outlines a method based on residues that leads to exact formulae, in a finite sum form, with no special functions, for evaluating P_{FA} and P_D (see Appendix A). Another approach consists in numerically implementing the steps in the Marcum-Swerling procedure above, using FFT's (Appendix B). Figs. 2.1-2.4 show some examples of P_D's vs R for different false alarms. For ease of comparison, the notation in [1] is used. As can be seen, the corresponding graphs are in excellent agreement.

The conclusions reached from investigating the residue (Appendix A) and FFT methods (Appendix B) are:

1. For Swerling I-IV targets the residue method is better in computing the probability of detection. However, there is a drawback: it is not suitable for complicated PDF's, since it may not be possible to compute the residuals analytically.

2. The FFT approach is better for Swerling 0 probabilities of detection. To achieve similar accuracy with the residue method, many terms of an infinite series have to be computed, leading to computer over/underflow. The FFT can also be used for arbitrary PDF's.

3. Both methods perform well for calculating the false alarm thresholds, with the FFT having the advantage for arbitrary PDF's.

4. The FFT method suffers from numerical round-off errors when calculating probability of detection for small peak-to-peak signal-to-noise ratios, R.

Clearly, another method is required for the calculation of probabilities of detection for arbitrary PDF's. This is the Monte Carlo method, discussed in the following section.

2.1   The Monte Carlo method

Often, in practice, the solution to a signal processing problem involving probabilities cannot be obtained analytically. In that case, the preferred approach to be taken is the Monte Carlo method. In this way, ensembles of the desired system can be constructed and, with suitable averaging, the desired probabilities estimated.

Swerling 0, N=1
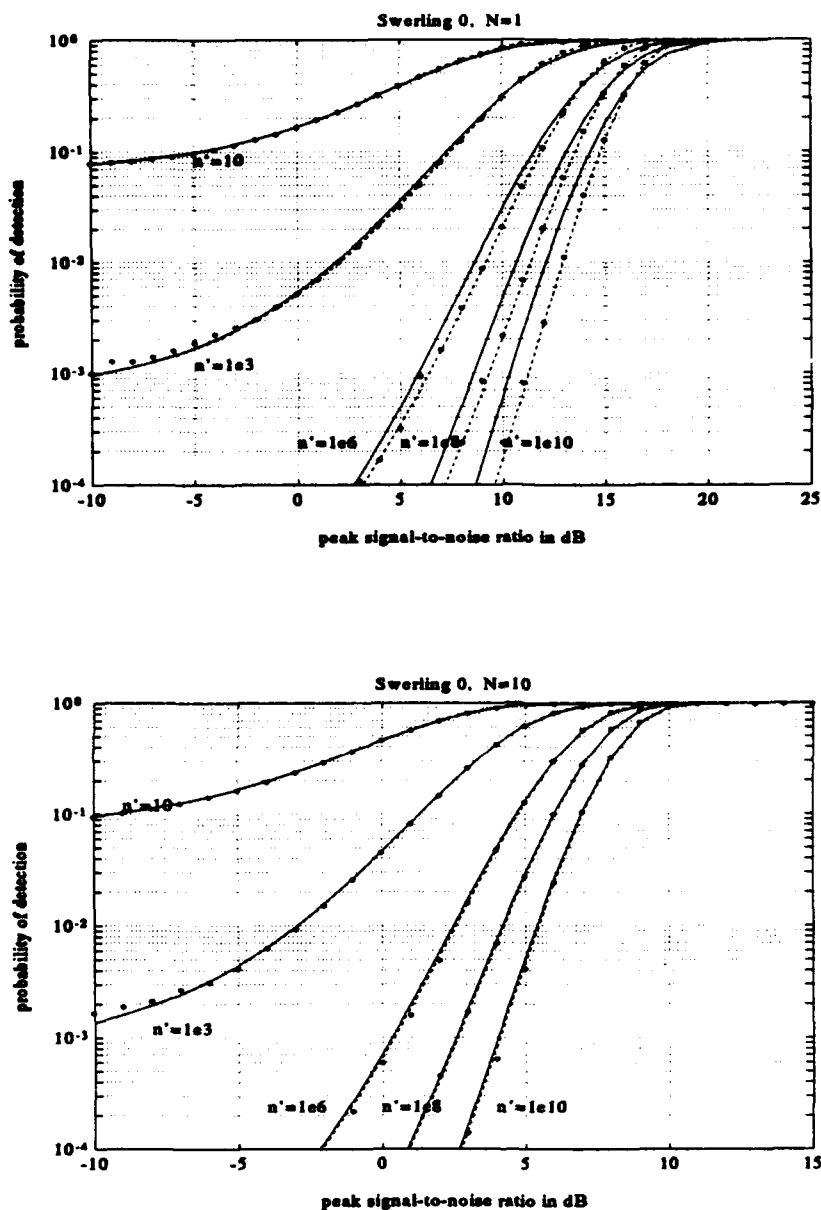
Swerling 0, N=10

Figure 2.1: Swerling 0, $N = 1$ (top graph) and $N = 10$ (bottom graph). N is the number of pulses incoherently integrated. The notation in DiFranco and Rubin is kept, where $P_{FA} = 0.693/n'$. Solid curves are computed with the residue method, dashed curves with the FFT and the $\star$'s with the Monte Carlo method. Note the excellent agreement between all methods in the bottom graph and the two lower P_{FA} cases in the top graph (two leftmost curves). The discrepancy in the other three cases in the top graph (three rightmost curves), between the residue approach and the other two methods, illustrates the difficulty of using an arbitrary large value of K terms in the residue sums (the theoretical value is $K = \infty$ for Swerling 0).
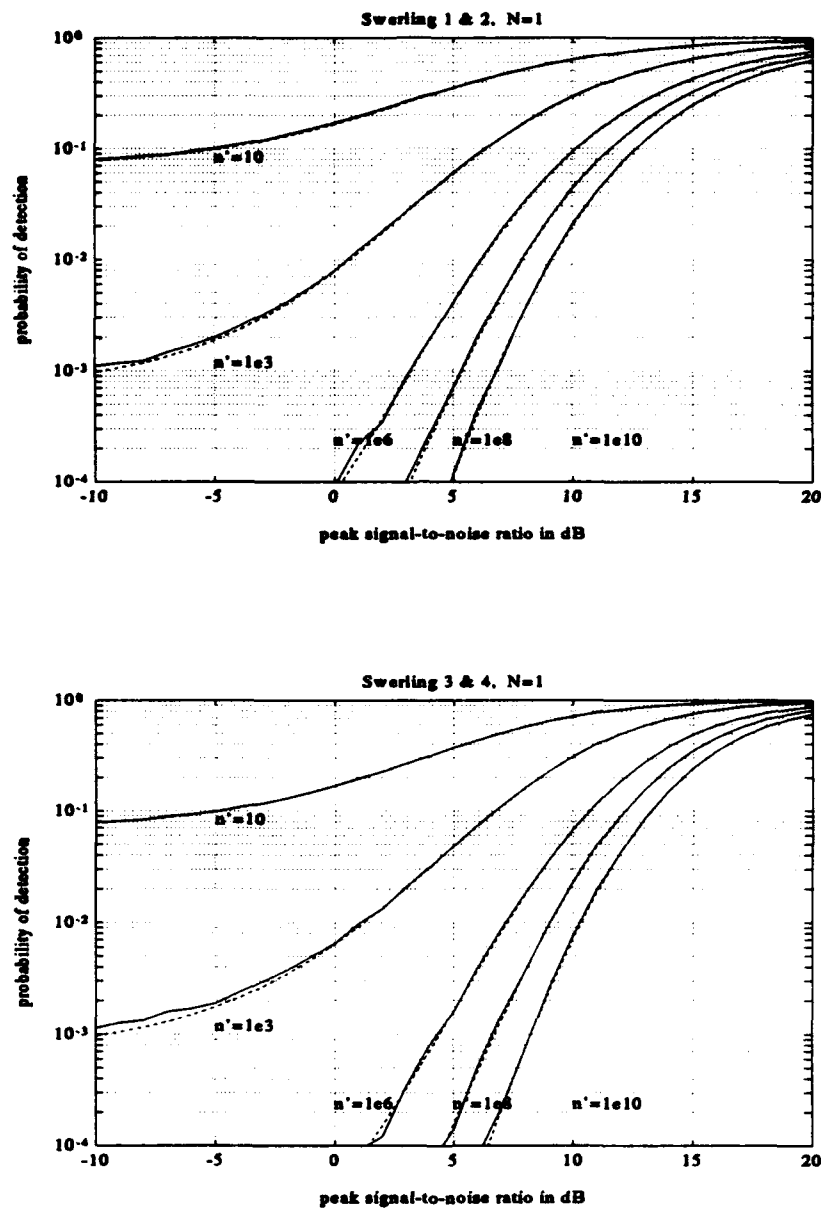
Figure 2.2: Swerling I and II, $N = 1$ (top graph) and Swerling III and IV, $N = 1$ (bottom graph). The solid curves are computed with the Monte Carlo method and the dashed curves are obtained with the residue method.
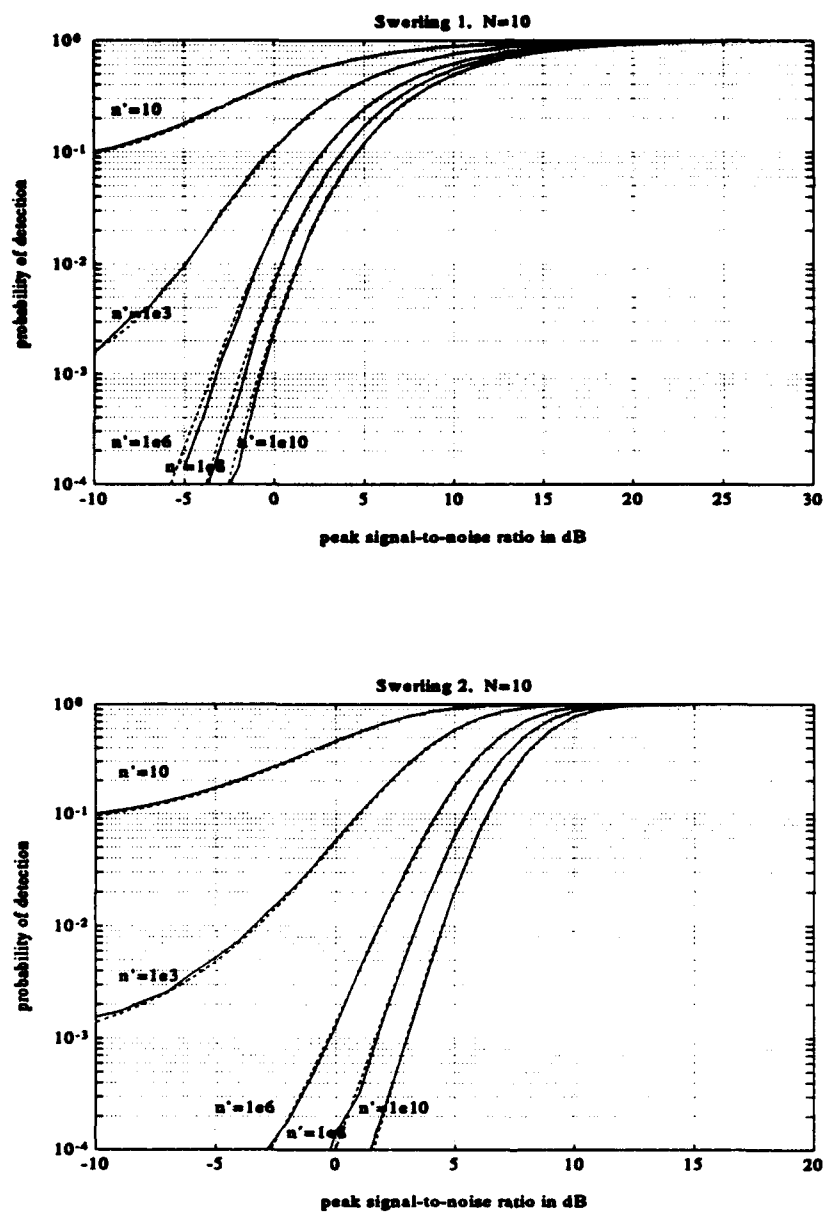
Figure 2.3: Swerling I, $N = 10$ (top graph) and Swerling II, $N = 10$ (bottom graph). The notation is the same as previously.
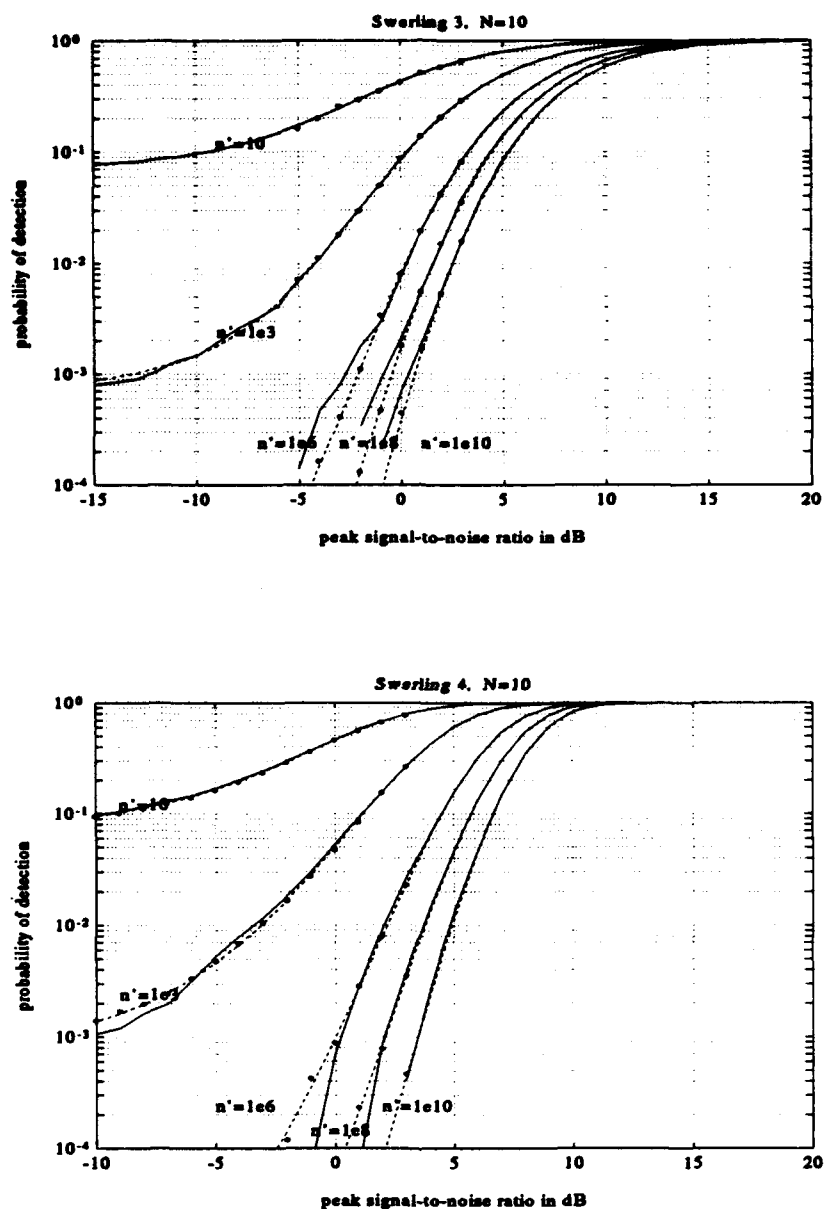
Figure 2.4: Swerling III, $N = 10$ (top graph) and Swerling IV, $N = 10$ (bottom graph). The notation is the same as previously. Importance sampling is implemented for the top graph, for peak signal-to-noise ratios between -5 dB to 3 dB, and, for the bottom graph for -10 dB to 3 dB. These cases are indicated with $\star$'s. In both cases, the accuracy is improved.

To estimate the probability of detection of a given signal, in a given noise background, with the Monte Carlo method, all that is needed is to find the correct way of generating the signal and noise samples. The receiver structure that simulates the necessary matched filter is easily coded in software and one only has to count how many times the test statistic (e.g. the squared envelope) exceeds the false alarm threshold.

In a straightforward implementation and without loss of generality, the simulated received signal component is the RF pulse,

$$s(t) = \begin{cases} A\cos(2\pi f_c t + \phi) & 0 \le t \le T_p \\ 0 & \text{otherwise} \end{cases} ,$$

where the pulse width, T_p, is equal to 2 time units, the carrier frequency $f_c = 3/T_p$, the sampling period $T_s = 0.2$ time units and the sampling rate $f_s = 1/T_s$. A is the signal amplitude, a constant for Swerling 0, and a Rayleigh or one dominant plus Rayleigh for the other Swerling cases. ϕ is the initial phase of the pulse, a uniformly distributed random variable in $[0, 2\pi]$. It turns out that 20 samples are enough to adequately describe the pulse per ensemble.

The matched filter with sampling at T_p is implemented with a digital correlator receiver, which approximates

$$\int_0^{T_p} r(t) \left\{ \begin{array}{c} I(t) \\ Q(t) \end{array} \right\} dt \quad \propto \quad \sum_{i=1}^{2f_s T_p} r_i \left\{ \begin{array}{c} I_i \\ Q_i \end{array} \right\} ,$$

where $I(t)$ and $Q(t)$ are the in-phase and quadrature components of the transmitted signal. The squared envelope is then taken, scaled by 1/2, leading to a single sample per pulse. For N integrated pulses, N samples are summed up for each sample of the test statistic.

Each test statistic sample is then compared with the appropriate threshold. If larger than the threshold, the probability of detection variable, P_D, (initial value 0) is incremented by $1/n_S$, where n_S is the number of ensembles used. The only problem is that, in order to adequately describe the rare events, that is, the tails of the distributions, n_S must be a very large number. This means that the code required to compute the statistic, although simple, may be extremely time consuming in execution.

2.2 Monte Carlo with importance sampling

A way to reduce the computational burden of the conventional Monte Carlo method, is to apply the technique of importance sampling. With importance sampling, one can modify the PDF(s) of the underlying distribution(s), so that the low probability events occur more frequently. The desired output probabilities are then found by appropriately weighting each event by a factor that depends only on the input state (Mitchell [4]).

The subject of interest in this report is the estimation of the probability of detection. Applying the Monte Carlo approach, the desired quantity to be estimated is the complement of the

Conventional Sampling
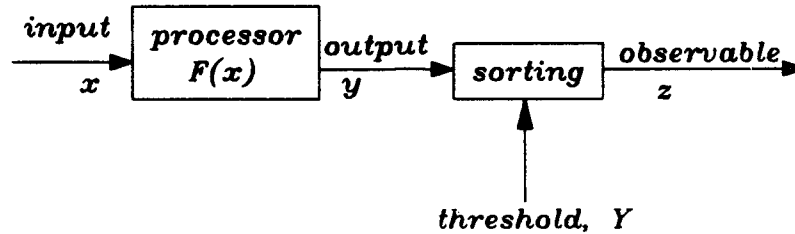
Importance Sampling
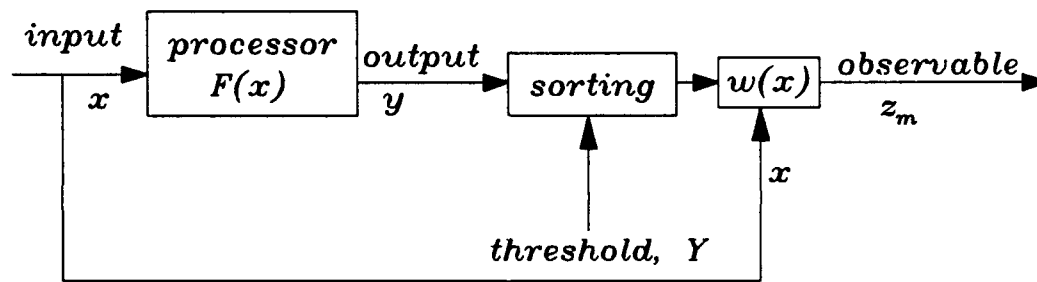
Figure 2.5: Sketch of operations performed with conventional and importance sampling.

Cumulative Distribution Function, CDF, of the test statistic

$$Q(y) = 1 - CDF(y) = \int_y^\infty p(x)dx \quad .$$

For a given false alarm threshold, y, the desired probability of detection is $Q(y)$. Or, in other words, for a desired probability of false alarm, P_{FA}, the appropriate false alarm threshold is $Q^{-1}(P_{FA})$. With conventional sampling, a value around $Q(y) = 10^{-6}$ requires a sample size at least as large as 10^6 in order to achieve any precision at all in the estimate. With importance sampling, the required sample size can drop by several orders of magnitude.

Fig. 2.5 sketches the operations performed with conventional and importance sampling. In conventional sampling, the input data process, x, multidimensional in general, enters the processor $F(x)$ and a one-dimensional output process y is generated, which for the example of y being the sum of N samples is given by $y = \sum_{i=1}^N x_i$, where x is an N-dimensional process. The process

y is sorted, with the sorting threshold Y, which varies from y_{min} to y_{max}. The function $Q(Y)$ is computed as the observable z. This is done by "binning" the sorted values into a histogram and computing the cumulative distribution function complement from it. In conventional sampling, the weight associated with each sample y is $w = 1$. In importance sampling, some parameter of the PDF of x is modified, to increase the occurrence of low probability events. The sorted samples y now receive the scalar weight

$$w(\mathbf{x}) = \frac{p(\mathbf{x})}{p_m(\mathbf{x})} \quad ,$$

which is the ratio of the original to the modified probability density functions.

2.2.1 Evaluating P_{FA}

In estimating the false alarm thresholds in Table 3.1, we have, as input, N samples x_i, each following the exponential distribution $\exp(-x_i)$. The input vector is

$$\mathbf{x} = (x_1, x_2, \ldots x_N)^T \quad ,$$

and the processor $F(\mathbf{x})$ simply adds the N components

$$y = F(\mathbf{x}) = \sum_{i=1}^{N} x_i \quad .$$

Assuming independent, identically distributed (i.i.d.) samples, the weight is

$$w(\mathbf{x}) = \prod_{i=1}^{N} \frac{\exp(-x_i)}{(1/\bar{x}_m)\exp(-x_i/\bar{x}_m)} = \bar{x}_m^N \exp[-y(1 - 1/\bar{x}_m)] \quad ,$$

where the parameter to be modified is the mean $\bar{x}$ of the individual exponential distributions, from the value 1 to $\bar{x}_m$. The original, unmodified, exponential variates are generated as

$$x_i = -\ln u \quad ,$$

where $u \sim U[0, 1]$ is a uniformly distributed random variable from zero to one, and the modified variates as

$$(x_i)_m = (-\ln u)\bar{x}_m \quad .$$

Fig. 2.6 shows $Q(Y)$ for $N = 1$ and $N = 10$, for 10,000 samples generated by conventional and importance sampling. Solving $Y = Q^{-1}(P_{FA})$ for a desired PFA, one can easily estimate the false alarm thresholds. Spline interpolation is used to generate a continuous function $Q(Y)$ from the binned samples, accurate enough for $Y \in [y_{min}, y_{max}]$. $Q(Y) - P_{FA} = 0$ is then solved for the desired threshold with the bisection method. The value $\bar{x}_m = 4.7$ used in the figure is optimized for $Q(Y) = 10^{-6}$. However, $Q(Y)$ is relatively insensitive to the exact value of the modifying parameter. Trying a variety of values, one usually observes that the estimates $Q(Y)$ cluster together. It should be emphasized that importance sampling is a technique designed to increase low-probability events. E.g., the curve $N = 10$, $\bar{x}_m = 4.7$ in Fig. 2.6 starts from $Y \sim 10$. For high probability events, $Q(Y) \sim 0.1 - 1$, it is advantageous to use conventional sampling.

2.2.2 Evaluating P_D

Mitchell [4] claims that the weight $w(\mathbf{x})$ depends only on the input $\mathbf{x}$ and is not affected by the processor $F(\mathbf{x})$. Note, however, his examples (5) and (6) where the processor outputs are:

$$y = \sum_{k=1}^{K} x_k$$

and

$$y = \sum_{k=1}^{K} a_k x_k \quad ,$$

respectively. The x_k's are exponentially distributed random variables in both examples. The only difference is the arbitrary coefficients a_k in the second. For both examples the weight, as a function of only the input, is the same, independent of the a_k's. The simulation results, however, show a larger error for the second case, for the same number of ensembles, n_S, used. This is compensated for by increasing n_S.

In our implementation of importance sampling, his example (9) is useful. A log-normally distributed random variable is combined there with thermal noise, which is Rayleigh-amplitude distributed. The processor output is the sum squared of the two inputs, typical for noncoherent radar systems.

Adapting this example to our case, the received signal, $r(t)$, is a sum of two phasors, V_s and V_n, the signal and noise phasors respectively, i.e.

$$r(t) = V_s + V_n = A\exp(j2\pi f_c t + \theta) + V_n \quad ,$$

where f_c is the carrier frequency and $\theta \sim U[0, 2\pi]$. The noise phasor, V_n, can be generated from a unit mean exponential distribution, leading to Gaussian noise, in-phase and quadrature components n_I and n_Q, of zero mean and variance $\sigma^2 = 1/2$. The envelope squared, x, [10, page 112] has the PDF

$$p(x) = \frac{1}{2\sigma^2}\exp\left[-\frac{1}{2\sigma^2}(x + A^2)\right] I_0\left(\frac{A\sqrt{x}}{\sigma^2}\right) \quad .$$

The amplitude of the sine wave, A, is scaled to the desired signal-to-noise-ratio (SNR), i.e. the magnitude of V_s is $\sqrt{R/2}$, where R is the peak-to-peak SNR. For Swerling 0, R is a constant. For Swerling 1 and 2, it is associated with a Rayleigh variable, i.e. R is exponentially distributed with mean $\bar{R}$, the mean peak-to-peak SNR. For Swerling 3 and 4, R is associated with the one-dominant-plus-Rayleigh distribution ($A_0 = (3\bar{R}/4)^{1/2}$, see [1]).

The method works well for all Swerling cases, and even improves the accuracy of the conventional Monte Carlo method that was illustrated in Fig. 2.4. Note that for Swerling's 0,1,2 and 3 cases, only 10,000 samples and 500 bins were required, as opposed to 100,000 samples for the conventional Monte Carlo method. However, the Swerling 4 case, even with importance sampling, did require 100,000 samples and 2,000 bins. Small values for the modifying parameters were adequate for all cases ($1 \leq \bar{x}_m \leq 2$). With larger values, the importance sampling CDF complement,

$Q(y)$ (Fig. 2.7), is seen to be stepwise rough, even with a small $\bar{x}_m$. In this regard, it is similar to Mitchell's example (6) mentioned earlier. The way to reduce the number of samples for case 4, is to increase both the bin size and the ensemble size, as was successfully done here.

2.3   Summary

In this section, the objective was to investigate and explore techniques for estimating the probability of detection for Swerling targets. It is desirable that the methodology developed should be able to handle, with relative ease, an arbitrary noise background and arbitrary probability densities for the signals. The known case of classic fixed threshold detection [1] is used as the comparison standard. The results of this investigation are:

1. The analytical method of residues works adequately for Swerling I-IV. It is less accurate for Swerling 0 and implementation is likely to be extremely complex for more complicated signal and noise PDF's (peak detection in K-distributed clutter). Therefore it is not pursued further, except as a conveniently fast way of checking different detection algorithms on the known white noise case.

2. The numerical FFT technique is of more general scope, capable of handling arbitrary PDF's. It is also very simple, in principle, to implement. However, for fluctuating targets, where R is a random variable, the numerical integrations involved are computationally extremely intensive. In addition, non-negligible numerical errors accumulate for lower SNR values. As such, it is of limited scope.

3. The Monte Carlo approach is the method of choice. The conventional implementation is very simple in concept, usually following the same patterns of operations as the hardware signal processing. As such, it is capable of handling arbitrary signal and noise backgrounds. To ease the computational burden for low-probability events, importance sampling may also be applied. Note that, contrary to the conventional Monte Carlo method, the importance sampling Monte Carlo method deals directly with the matched filter outputs instead of estimating them with a correlator receiver structure. This makes software coding much simpler to implement.

The Monte Carlo method, with importance sampling when appropriate, is the technique used in the following investigation.
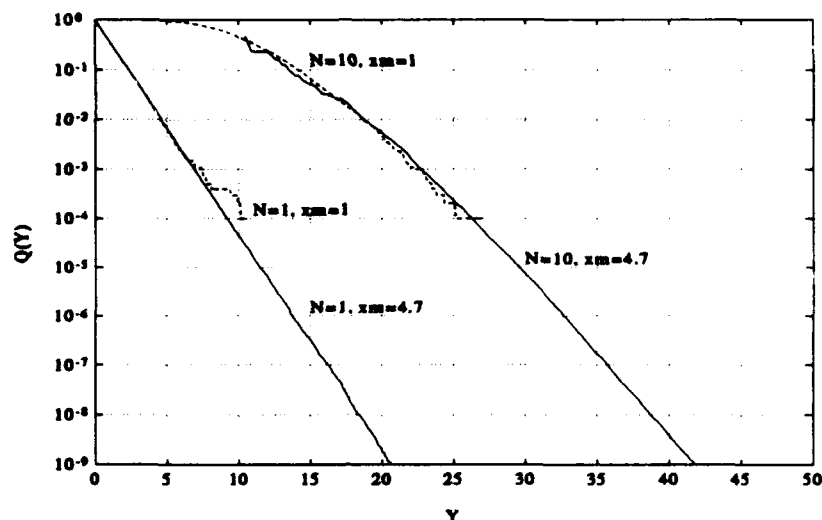
Figure 2.6: An example of conventional and importance sampling. Solid lines refer to importance sampling, optimized for $Q(Y) = 10^{-6}$ with $\bar{x}_m = 4.7$ and dashed lines to conventional sampling.
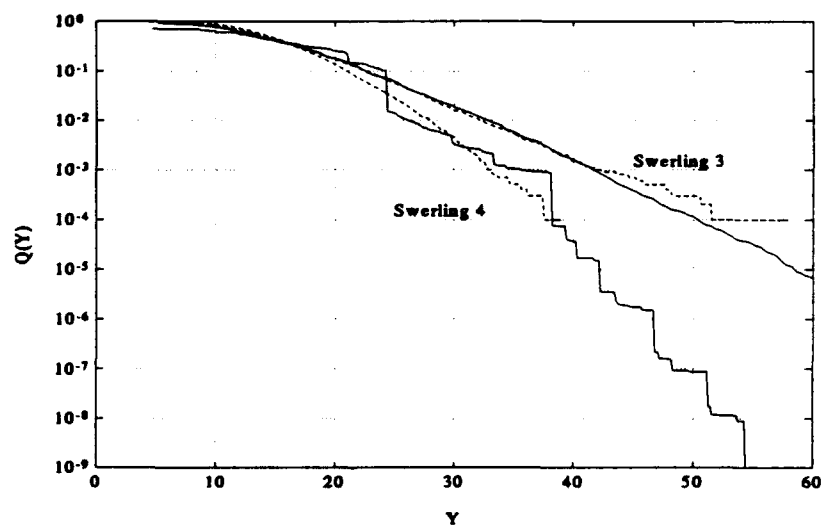
Figure 2.7: The cumulative distribution function complement, $Q(Y)$, for Swerling 3 and 4, $N = 10$, $\bar{R} = 0$ dB, with conventional (dashed) and importance sampling (solid), with $\bar{x}_m = 1$ and 1.5 respectively. Note the behaviour for Swerling 4. By increasing the sample size from 10^4 to 10^5 and the bin size from 500 to 2,000, the "staircase" for Swerling 4 becomes as smooth as for Swerling 3.

3

Peak detection in white noise

In peak detection, we consider a set of $N \times m$ independent samples. We extract the peak value from each consecutive subset of m samples, collapsing the $N \times m$ samples into N. The PDF of the collapsed samples, $p_{(m)}(x)$, is that of the mth order statistic [5, page 175]

$$p_{(m)}(x) = mF_x^{m-1}(x)p_x(x) \quad ,$$

where F_x and p_x are the CDF and PDF, of the original samples, respectively.

In order to analytically estimate the false alarm thresholds for a single observation ($N = 1$) in white noise, the PDF and CDF of the original samples are defined as

$$p(x;0) = e^{-x} \qquad \text{for } x \geq 0$$

and

$$F_x(x;0) = \int_0^x e^{-t}dt = 1 - e^{-x} \qquad \text{for } x \geq 0 \quad ,$$

respectively. The mth order statistic PDF therefore becomes

$$p_{(m)}(x;0) = m(1 - e^{-x})^{m-1}e^{-x} \qquad x \geq 0 \quad .$$

It is now straightforward to evaluate the CDF complement

$$Q(y) = m \sum_{k=0}^{m-1} (-1)^k \binom{m-1}{k} \frac{\exp[-(k+1)y]}{k+1}$$

and the exact false alarm thresholds

$$T_{FA} = -\ln\left(1 - \sqrt[m]{1 - P_{FA}}\right)$$

for $N = 1$. The latter can be used to validate the Importance Sampling, IS, thresholds for $N = 1$ (Table 3.2), and provide confidence in the results for $N > 1$, where IS is the only feasible method. In Figs. 3.1–3.2, we see the estimated $Q(y)$'s for both conventional and importance sampling Monte

Carlo. For comparison, the case for $m = 1$, corresponding to no peak detection, is included in the figure.

Figs. 3.3 - 3.6 show the peak detection, P_D's, vs the peak SNR, R. For comparison, the corresponding P_D's for classic fixed threshold detection, for $N \times m$ and N integrated pulses, are also displayed.

Table 3.1: Classic fixed threshold method false alarm thresholds, T_{FA}, for various values of n', computed with the residue (R), the FFT (F) and the Monte Carlo (MC) method. The size of the FFT is 8192 for the F($N = 1$) column and 16384 for the F($N = 10$) column, and the maximum upper bound used in the integration is $u_b = \text{nFFT} \times \Delta x$. The MC method uses importance sampling on exponentially distributed variables, with $\bar{z}_m = 10\bar{z}$ and $\bar{z}_m = 4\bar{z}$ for the two columns respectively, where $\bar{z} = 1$ is the mean of the unmodified exponential distribution.

n'	R ($N = 1$)	R ($N = 10$)	F ($N = 1$)	F ($N = 10$)	MC ($N = 1$)	MC ($N = 10$)
10	2.669	15.017	2.669	15.046	2.690	15.099
10^3	7.274	23.238	7.274	23.253	7.271	23.224
10^6	14.182	33.208	14.182	33.216	14.168	33.119
10^8	18.787	39.271	18.787	39.278	18.787	39.288
10^{10}	23.392	45.084	23.392	45.090	23.350	45.090

Table 3.2: Peak detection method false alarm thresholds, T_{FA}, for various values of n', computed with the Monte Carlo (MC) method with importance sampling. For comparison, the analytically derived values (A) for $N = 1$ are given as well.

| n' | $N = 1$ | | | | $N = 10$ | |
| | $m = 5$ | | $m = 10$ | | $m = 5$ | $m = 10$ |
	A	MC	A	MC	MC	MC
10	4.250	4.238	4.940	4.912	28.718	35.277
10^3	8.884	8.877	9.577	9.621	37.499	44.041
10^6	15.792	15.660	16.485	15.699	47.699	53.657
10^8	20.397	20.338	21.090	20.939	53.899	60.197
10^{10}	25.002	24.913	25.695	24.663	59.401	64.542
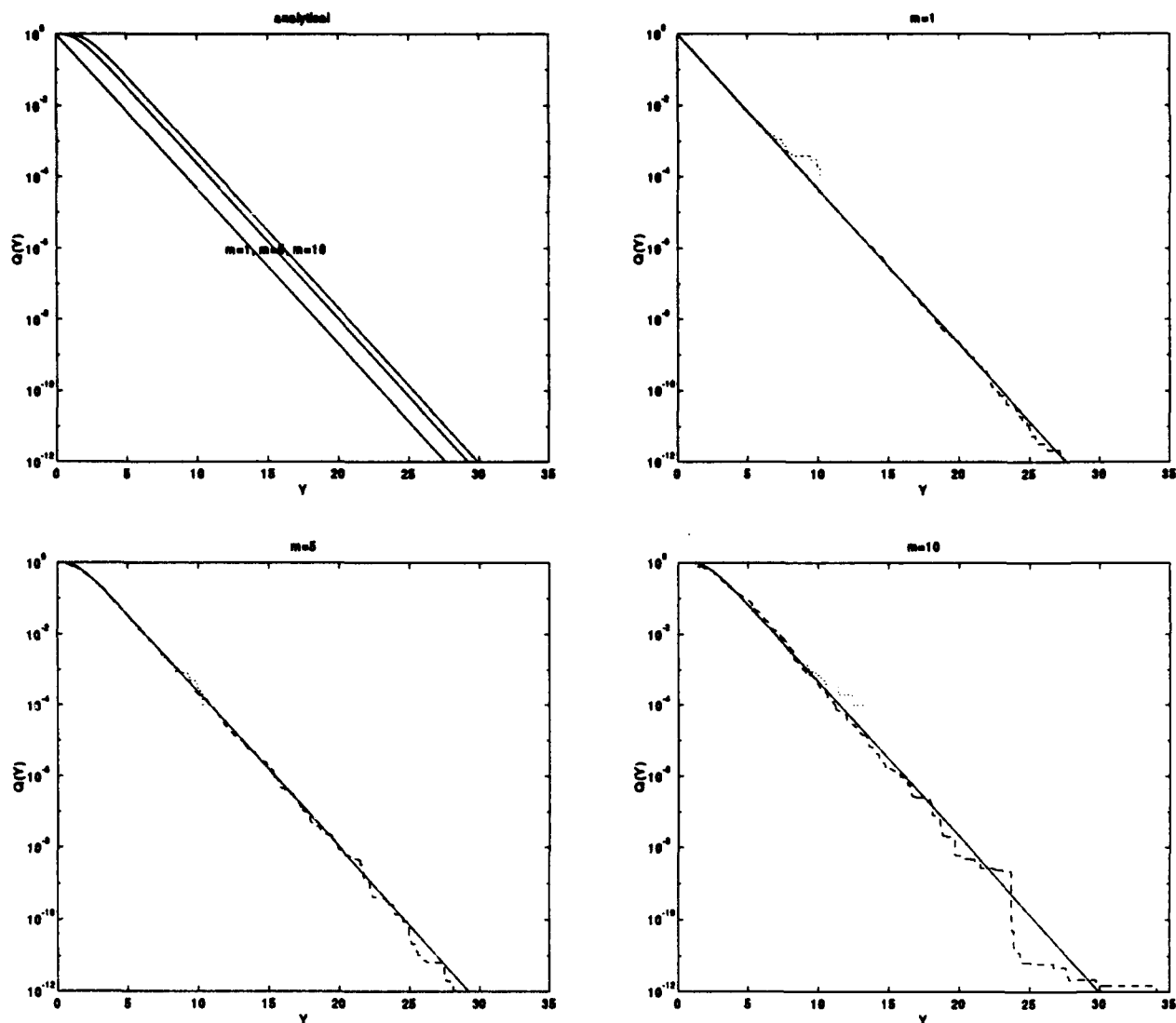
Figure 3.1: The cumulative distribution function complements, $Q(Y)$, for the noise-only case in peak detection, for $N = 1$. The top left graph displays the analytical $Q(Y)$'s. The top right graph displays the case $m = 1$; analytical formula (solid line); importance sampling (dashed line); conventional sampling (dotted line). Note that conventional sampling ends at $Q(Y) \sim 10^{-4}$ since the ensemble size is 10^4. The bottom graphs follow the same conventions as the top right graph, for the cases $m = 5$ and $m = 10$. These curves are used to derive the false alarm thresholds for various m.
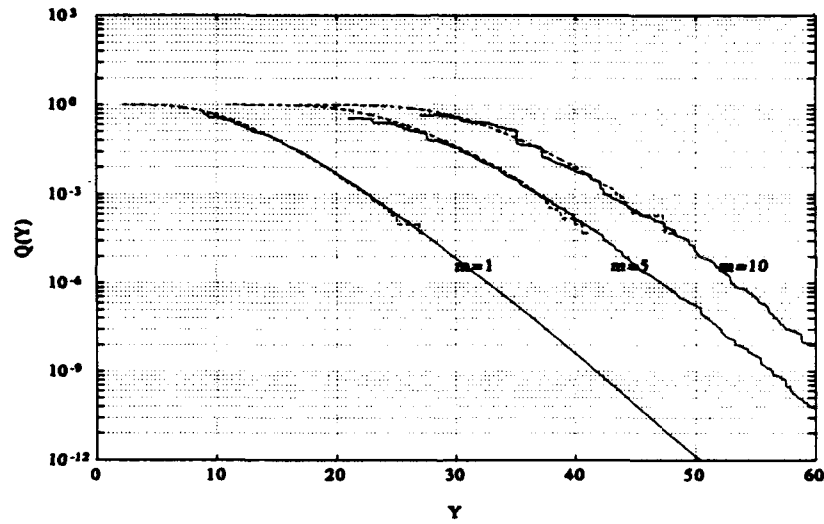
Figure 3.2: The cumulative distribution function complements, $Q(Y)$, for the noise-only case in peak detection, for $N = 10$. The dashed line corresponds to conventional sampling; importance sampling is represented by the solid line. These curves are used to derive the false alarm thresholds for various m. This is done by first choosing the desired P_{FA} on the vertical $Q(Y)$ axis and then reading the corresponding T_{FA} on the Y axis.
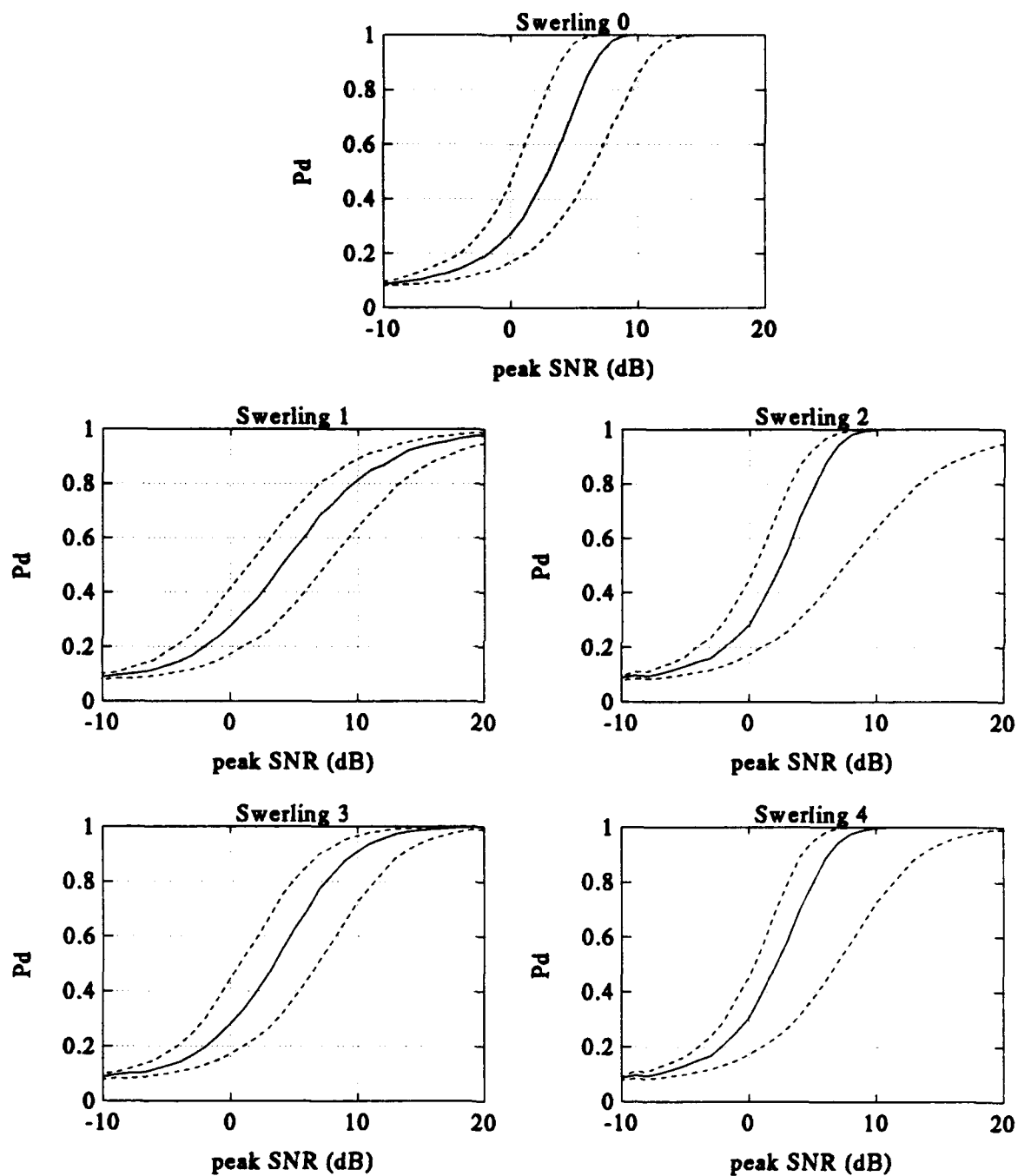
Figure 3.3: Probabilities of detection for $n' = 10$. The solid curve is for $N = 1$, $m = 10$ peak detection, and the dashed curves are for $N = 10$ (upper) and $N = 1$ (lower) classic fixed threshold detection, respectively. At $P_D = 0.5$, the loss for the peak detected method vs the optimum $N \times m$ is about 2.5 dB or less.
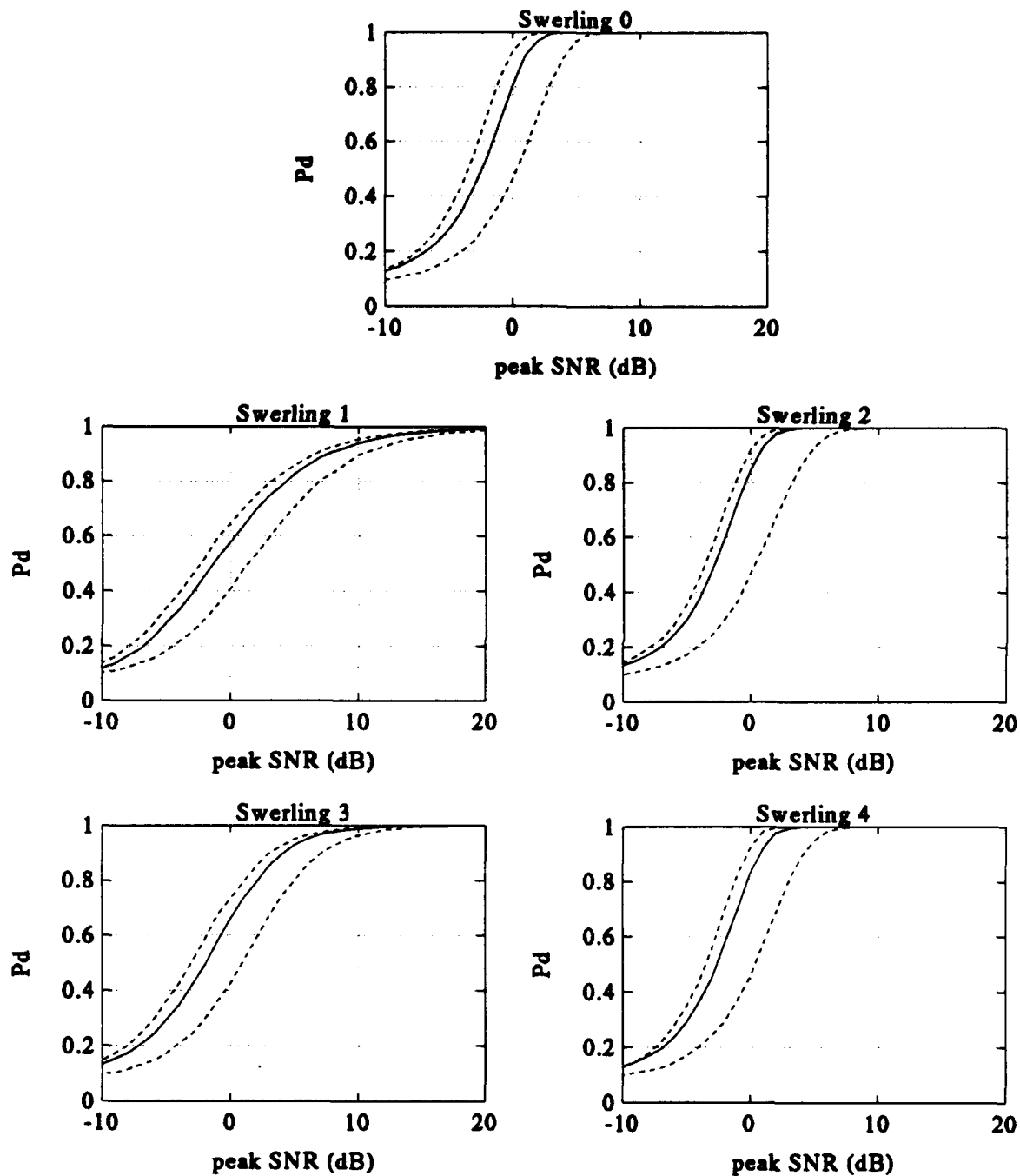
Figure 3.4: Probabilities of detection for $n' = 10$. The solid curve is for $N = 10$, $m = 5$ peak detection, and the dashed curves are for $N = 50$ (upper) and $N = 10$ (lower) classic fixed threshold detection, respectively. At $P_D = 0.5$, the loss for the peak detected method vs the optimum $N \times m$ is about 1 dB or less.
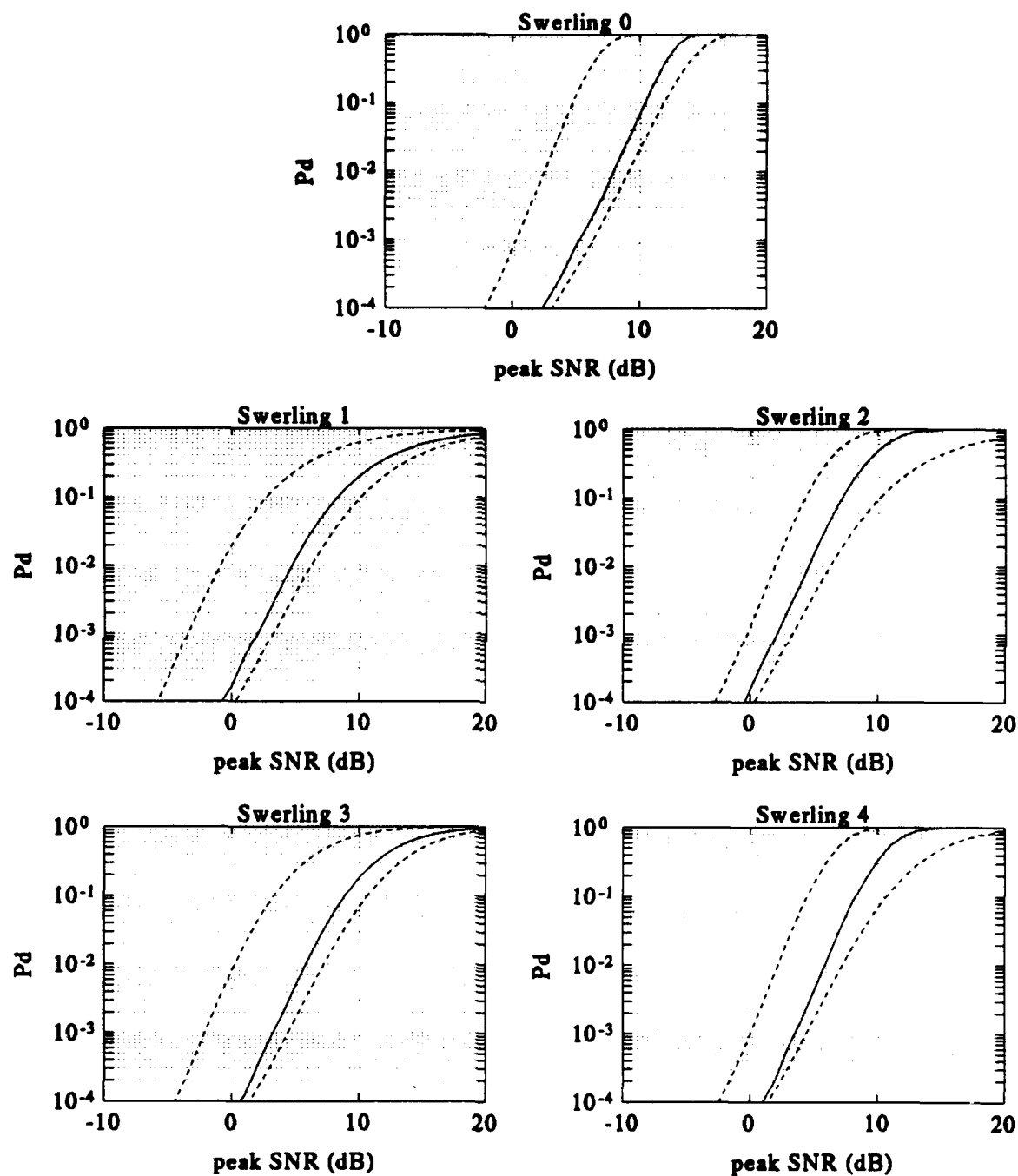
Figure 3.5: Probabilities of detection for $n' = 10^6$. The solid curve is for $N = 1$, $m = 10$ peak detection, and the dashed curves are for $N = 10$ (upper) and $N = 1$ (lower) classic fixed threshold detection, respectively. At $P_D = 0.5$, the loss for the peak detected method vs the optimum $N \times m$ is about 5.5 dB or less.
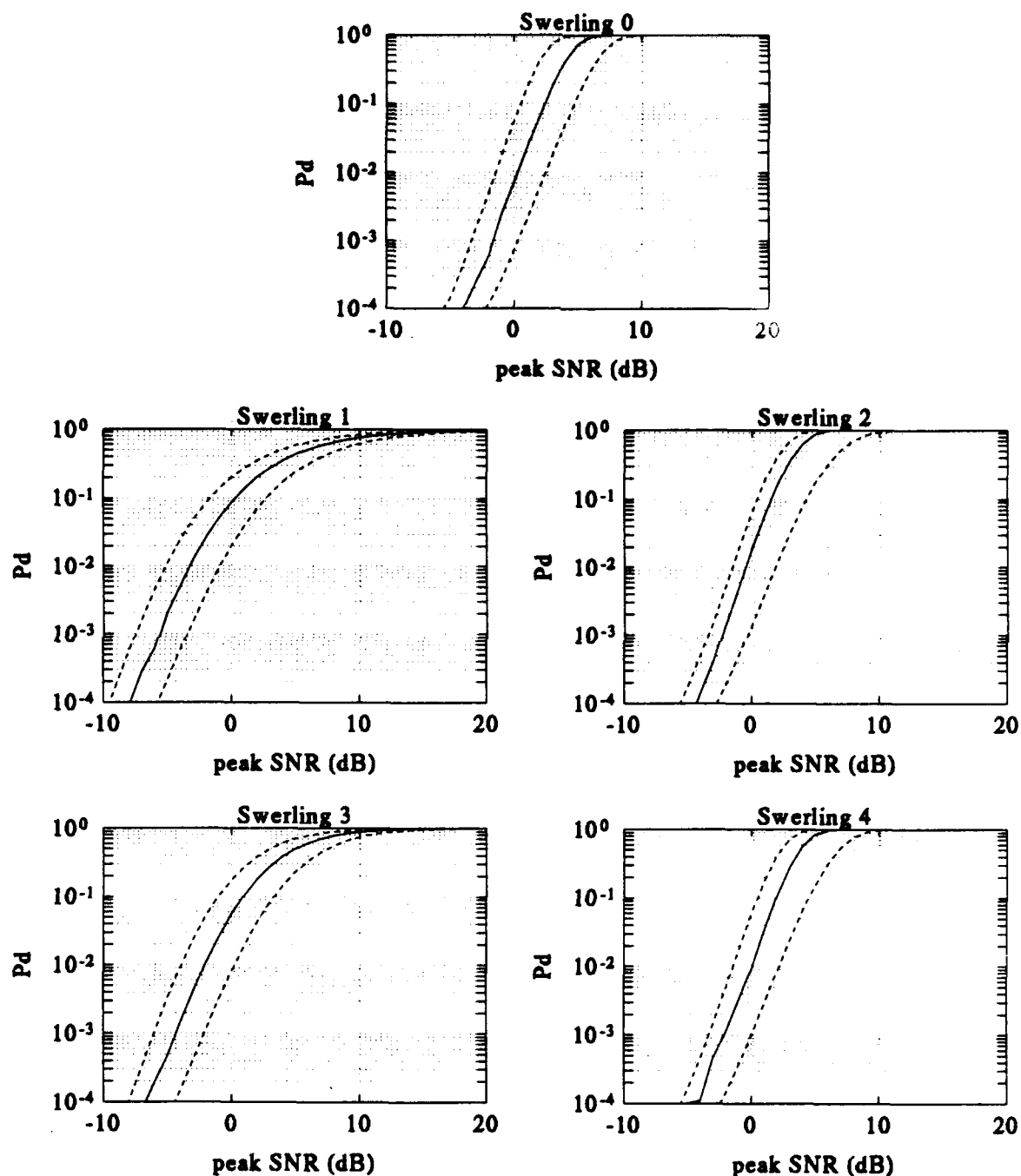
Figure 3.6: Probabilities of detection for $n' = 10^6$. The solid curve is for $N = 10$, $m = 5$ peak detection, and the dashed curves are for $N = 50$ (upper) and $N = 10$ (lower) classic fixed threshold detection, respectively. At $P_D = 0.5$, the loss for the peak detected method vs the optimum $N \times m$ is about 2 dB or less.

4

Conclusions and future work

At this point, following the peak detection investigation, the following progress has been made:

- The methodology for evaluating peak detection performance of arbitrary signal and noise/clutter structures has been developed. The method that was chosen is the Monte Carlo method with importance sampling.

- Peak detection, P_D's vs R, curves have been computed for all Swerling type targets in a white noise background, for certain cases of the parameters N, m and n'. These have been compared to classic threshold detection performance and, as expected, there was a loss of the order of a few dB's, that depends on the choice of the above parameters.

    The work that remains to be done is:

1. To complete the investigation of peak detection performance in a white noise background for a specific radar system, e.g. a radar suitable for periscope detection [8]. The effects of bandwidth reduction and collapsing losses will be examined and the overall detection performance established.

2. The noise/clutter background will be extended to cover K-distributed clutter. This is the commonly accepted model used to describe sea clutter statistics.

3. Finally, noise/clutter correlation aspects will be investigated, together with the design of the proper prewhitening filters.

Appendix A

Residue method

The residue method, as developed by Hou et al. [2], leads to exact formulae, in a finite sum form and with no special functions, for evaluating P_{FA} and P_D.

Given the test statistic, x, with PDF, $p(x)$, they extend the characteristic function of x (see [5]),

$$\Phi(\omega) = \int_{-\infty}^{\infty} p(x)e^{j\omega x} dx \quad ,$$

by replacing the imaginary variable $j\omega$ with the complex variable $-z$. The modified characteristic function is called the Moment Generating Function, MGF, in essence a double-sided Laplace transform:

$$C(z) = \int_{-\infty}^{\infty} p(x)e^{-zx} dx \quad .$$

The residue theorem can then be used to compute

$$p(x) = \sum_{k} \text{res}[C(z)e^{zx}; z_k] \quad ,$$

where the poles z_k are in the left half-plane when $x > 0$, and in the right half-plane when $x < 0$. With this approach,

$$\int_{T}^{\infty} p(x)dx = -\sum_{k} \text{res}[C(z)\frac{e^{bz}}{z}; z_k] \quad ,$$

where $T > 0$ and $x > 0$, and

$$P_{FA} = \int_{T_{FA}}^{\infty} p(x; 0)dy = -\sum_{k0} \text{res}[C_0(z)\frac{e^{T_{FA}z}}{z}; z_{k0}] \quad ,$$

$$P_D = \int_{T_{FA}}^{\infty} p(x; R)dx = -\sum_{k1} \text{res}[C_1(z)\frac{e^{T_{FA}z}}{z}; z_{k1}] \quad ,$$

where z_{k0} and z_{k1} are the respective poles of $C_0(z)$ and $C_1(z)$ lying in the left half-plane, and R is the peak SNR.

The χ^2 family of fluctuating targets have the PDF

$$p(R) = \frac{1}{\Gamma(K)} \left(\frac{K}{\bar{R}}\right)^K R^{K-1} \exp(-KR/\bar{R}) \quad ,$$

where $\bar{R}$ is the average of R over target fluctuation and $K > 0$ is a fluctuation parameter. The values $K = 1, N, 2, 2N$ and $K = \infty$ correspond to the Swerling cases I,II,III,IV and 0, respectively.

A.1 Evaluating P_{FA}

The MGF for the random variable x_i (single observation) for the case of noise only, is

$$C_i(z) = \int_{-\infty}^{\infty} p(x_i; 0)e^{-zx_i}dx_i = \int_0^{\infty} e^{-(1+z)x_i}dx_i = \frac{1}{1+z} \quad .$$

The MGF for x (N observations) is

$$C(z) = \prod_{i=1}^{N} C_i(z) = \frac{1}{(1+z)^N}$$

and the threshold, T_{FA}, for a given probability of false alarm, can be computed from[1]

$$P_{FA} = - \text{res}\left[C(z)\frac{e^{T_{FA}z}}{z}\right] = -\frac{1}{(N-1)!} \lim_{z \to -1} \frac{d^{N-1}}{dz^{N-1}}\left[(z+1)^N C(z)\frac{e^{T_{FA}z}}{z}\right] = \sum_{n=0}^{N-1} \frac{T_{FA}^n \exp(-T_{FA})}{n!} \quad .$$

In the present report, the numerical evaluation of the root of

$$f(T_{FA}) = \sum_{n=0}^{N-1} \frac{T_{FA}^n \exp(-T_{FA})}{n!} - P_{FA}$$

is done with the bisection method [6], double precision arithmetic and a relative accuracy of 10^{-12}.

A.2 Evaluating P_D

When a target is present, $R \neq 0$, and the MGF for the nonfluctuating case (Swerling 0) is[2]

$$C(z|R) = \frac{1}{(1+z)^N} \exp\left[-\frac{NRz}{2(1+z)}\right] \quad .$$

---

[1]Use is made of the formula

$$\frac{d^{N-1}}{dz^{N-1}}[\Phi(z)e^{zz}] = \sum_{n=0}^{N-1} \binom{N-1}{n} \left[\frac{d^{N-1-n}}{dz^{N-1-n}}\Phi(z)\right]\left[\frac{d^{N-1}}{dz^{N-1}}e^{zz}\right]$$

[2]Use is made of [7, page 306]

$$\int_0^{\infty} x\exp(-bx^2)I_0(cx)dx = \frac{1}{2b}\exp\left(\frac{c^2}{4b}\right)$$

The unconditional MGF for the fluctuating case is

$$C(z) = \int_0^\infty C(z|R)p(R)dR = \frac{(1+z)^{K-N}}{[1+(1+N\bar{R}/2K)z]^K} \quad .$$

For $1 \le K < N$, there is an $(N-K)$th order pole at $z_1 = -1$ and a Kth order pole at $z_2 = -F$, where $F = 1/(1+N\bar{R}/2K)$, so that

$$P_D = \sum_{n=0}^{N-K-1} \binom{N-n-2}{K-1} \frac{(-F)^K \exp(-T_{FA})}{G^{N-n-1}} \sum_{\ell=0}^{n} \frac{T_{FA}^\ell}{\ell!}$$

$$+ \sum_{m=0}^{K-1} \binom{N-m-2}{N-K-1} \frac{(-F)^{K-m-1}}{G^{N-m-1}} \exp(-FT_{FA}) \sum_{\ell=0}^{m} \frac{(FT_{FA})^\ell}{\ell!}$$

with $G = 1 - F$. For $1 \le N \le K$, there is only a Kth order pole at $z = -F$ and the detection probability becomes

$$P_D = \sum_{m=N-1}^{K-1} \binom{K-N}{K-m-1} \frac{F^{K-m-1}}{G^{N-m-1}} \exp(-FT_{FA}) \sum_{\ell=0}^{m} \frac{(FT_{FA})^\ell}{\ell!} \quad .$$

Using the above relations, the classic Swerling curves can be computed in a straightforward manner. Note, however, that large factorials can overwhelm the capability of the computer, especially for the Swerling 0 case, where $K = \infty$. For low values of N, putting $K = 10N$ is usually sufficient. Since we are mostly interested in ratios of factorials, computer limitations are also reduced by using $\ln \Gamma$, for which efficient code exists in [6], and exploiting the relation of the gamma function $\Gamma(z) = (z-1)!$.

Appendix B

The FFT method

An alternative approach for evaluating the integrals for P_{FA} and P_D is to do it directly, with FFT's. The main steps in this procedure are:

1. Prepare a table of values for the individual PDF, $p(x_i; R)$.

2. Use the FFT to transform to the frequency domain. This is equivalent to computing the characteristic function of the random variable x_i.

3. Raise the Fourier transformed sequence to the power N to take into account the integration of N observations. The PDF of the sum of a sequence of random variables is the convolution of the individual PDF's. This convolution is transformed to multiplication in the frequency domain.

4. Compute the inverse FFT of the obtained result. This should be a table of values of the sum PDF, $p(x; R)$, where $x = \sum_{i=1}^{N} x_i$.

5. Use spline interpolation to find function values at arbitrary points in the region of interest, allowing the numerical computation of the threshold root and the integrals for P_{FA} and P_D.

There is a trade-off here: the FFT sampling has to be fine enough, and the sample size large enough, to adequately describe the relevant functions in the domain of interest. This makes necessary the careful checking of the PDF's involved, i.e. there is a need to make sure that the area under the PDF curve is one and that no aliasing occurs to distort the PDF. For large values of N, the size of the FFT can become prohibitively large.

When we apply this technique to the known case of classic fixed threshold detection for all Swerling type targets, we have the situation described below.

B.1 Evaluating P_{FA}

The probability of false alarm, P_{FA}, for the non-fluctuating target, is identical in all Swerling cases, since the PDF for the noise-only case is unaffected by assumptions about the signal. The individual PDF for a single observation is:

$$p(z_i) = \begin{cases} \exp(-z_i) & z_i \geq 0 \\ 0 & z_i < 0 \end{cases}, \qquad (B.1)$$

while that for N observations is:

$$p(x) = \begin{cases} x^{N-1}\exp(-x)/(N-1)! & x \geq 0 \\ 0 & x < 0 \end{cases}. \qquad (B.2)$$

Fig. B.1 shows the results of the FFT method applied to (B.1). The comparison with the exact PDF (B.2), for the two cases shown, is almost exact, except for the overshoot around the peak. This suggests that the numerical quadrature should be performed on the right tail of the PDF with the integration limits from an unknown threshold to a maximum upper bound. Table 3.1 compares the residue approach thresholds with the FFT derived ones. As can be seen, agreement is excellent.

B.2 Evaluating P_D

For the evaluation of P_D, the FFT method fails to perform in a completely satisfactory manner. Even though there is no problem in computing PDF's for an arbitrary peak signal-to-noise ratio R, the PDF's are conditional upon R, which is now a random variable that must be integrated out. If one places the conditional PDF values in the columns of an array, the rows, as functions of R, must be multiplied by the PDF of R and integrated. A $10,000 \times 10,000$ array was used for Fig. B.2 (requiring a look-up table of several Mbytes) and as can be seen, the numerical errors that accumulate for low SNR's are too large to be ignored.
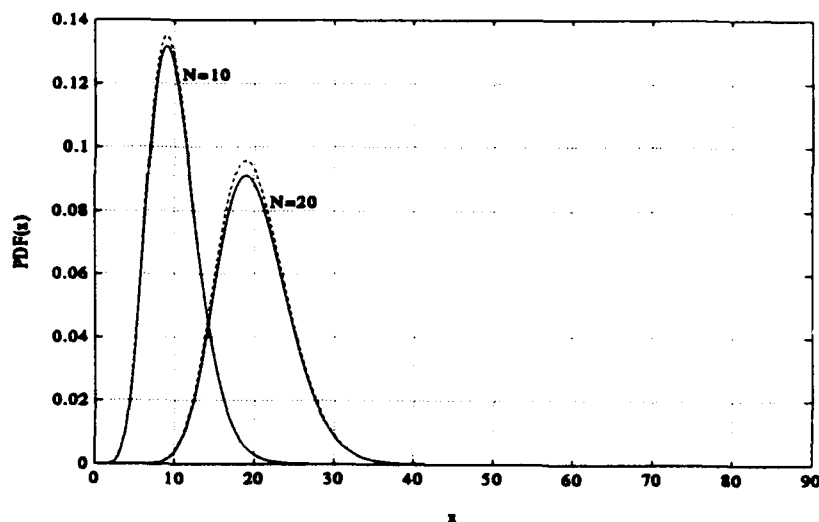
Figure B.1: Comparison of the exact, noise-only PDF (solid line) for arbitrary N, with the FFT derived one, based on $N = 1$ (dashed line). Two cases are shown, $N = 10$ and $N = 20$. The FFT step is $\Delta x = 5 \times 10^{-3}$ for both cases, and the FFT size is 8192 and 16384, respectively. In general, a larger FFT size leads to less overshoot. However, the discrepancy is less important in the tails, where the match between the two curves is almost exact.

Figure B.2: This is the "death" blow for the FFT method for Swerling I to IV. For lower SNR values, the numerical errors accumulated in the integrations involved can no longer be ignored. (Solid curves are computed with the FFT method, dashed curves with the residue).

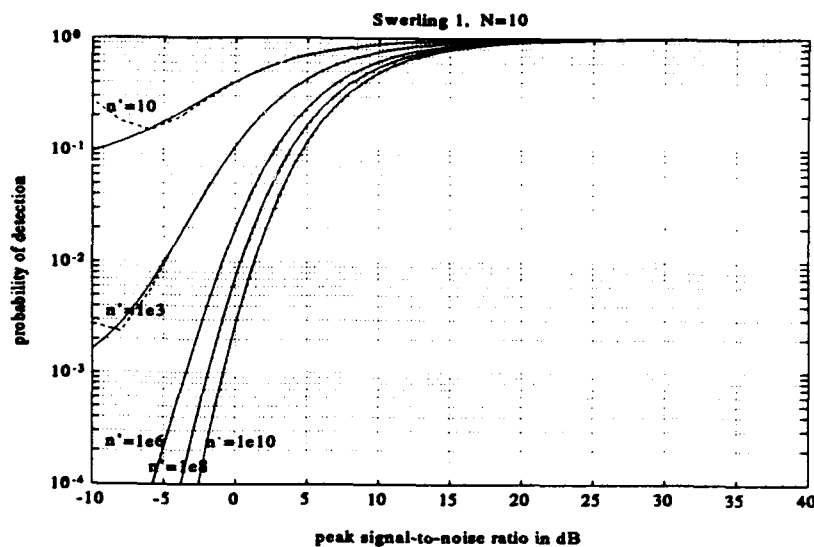# Appendix C

Generation of Rayleigh and 1-dominant-plus-Rayleigh random variables

The Rayleigh PDF is

$$p(A) = \frac{A}{A_0^2} \exp\left(-\frac{A^2}{2A_0^2}\right)$$

for $A \geq 0$. Rayleigh random variates can be generated by

$$A = \sqrt{x_1^2 + x_2^2} \quad,$$

where x_1 and x_2 are zero-mean Gaussian random variables with root variance $\sigma = A_0$. They can also be generated from an exponential distribution with mean $2A_0^2$ as

$$A = \sqrt{(-\ln u)2A_0^2} \quad,$$

where $u \sim U[0,1]$.

The one-dominant-plus-Rayleigh PDF is

$$p(A) = \frac{9A^3}{2A_0^4} \exp\left(-\frac{3A^2}{2A_0^2}\right)$$

for $A \geq 0$ and they can be generated as follows: Using the transformation method in [6, pages 200-201], a random variable $u \sim U[0,1]$ can be transformed to a one-dominant-plus-Rayleigh x by solving

$$e^{ax^2}(1 + ax^2) = 1 - u$$

for x, where $a = 3/(2A_0^2)$. This can be put in the form $f(z) = z$ and solved iteratively, i.e.

$$\ln\left(\frac{1+z}{1-u}\right) = z \quad,$$

34

where $z = ax^2$. The histogram from 1000 random variables generated this way, together with the analytical PDF for $A_0 = 2$, are shown in Fig. C.1. The application of importance sampling is shown in Fig. C.2, where the modifying parameter is now A_0.
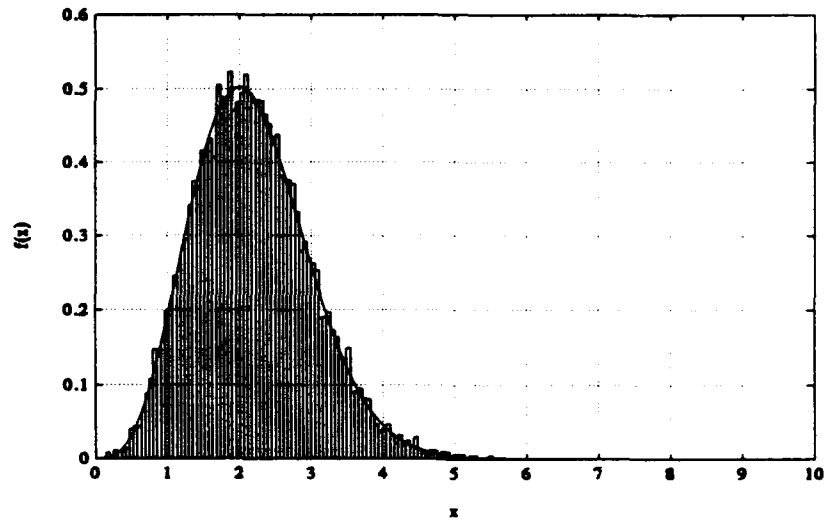
Figure C.1: The histogram from 1000 one-dominant-plus-Rayleigh random variables, together with the analytical PDF, for $A_0 = 2$.
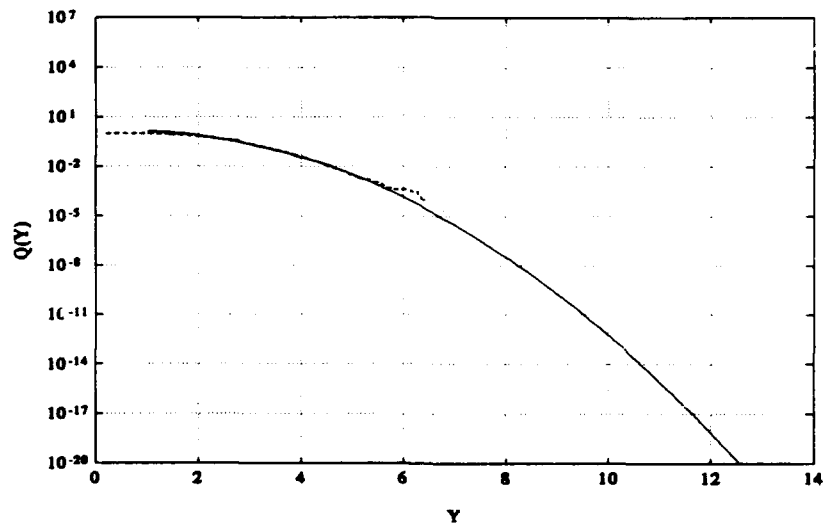

Figure C.2: The cumulative distribution function complement $Q(Y)$ for the one-dominant-plus-Rayleigh random variable, with conventional (dashed) and importance sampling (solid). 10,000 samples and 500 bins were used with $\bar{x}_m = 5$ for importance sampling.

References

[1] J.V. DiFranco and W.L. Rubin. *Radar Detection*. Artech House, 1980.

[2] X.Y. Hou, N. Morinaga, and T. Namekawa. Direct evaluation of radar detection probabilities. *IEEE Trans. Aerospace and Electronic Systems*, AES-23:418–424, 1987.

[3] J.I. Marcum. A statistical theory of target detection by pulsed radar. *IRE Trans. on Information Theory*, IT-6:59–267, 1960.

[4] R.L. Mitchell. Importance sampling applied to simulation of false alarm statistics. *IEEE Trans. Aerospace and Electronic Systems*, AES-17:15–24, 1981.

[5] A. Papoulis. *Probability, Random Variables, and Stochastic Processes*. Mc-Graw Hill, 2nd edition, 1984.

[6] W.H. Press, B.P. Flannery, S.A. Teukolsky, and W.T. Vetterling. *Numerical Recipes*. Cambridge Univeristy Press, 1986.

[7] A.P. Prudnikov, Y.A. Brychkov, and O.I. Marichev. *Integrals and Series, Vol II, Special Functions*. Gordon and Breach Science Publishers, 1986.

[8] J.M. Smith and R.H. Logan. An/aps-116 periscope detecting radar. *IEEE Trans. Aerospace and Electronic Systems*, AES-16:66–73, 1980.

[9] P. Swerling. Probability of detection for fluctuating targets. *IRE Trans. on Information Theory*, IT-6:269–300, 1960.

[10] A.D Whalen. *Detection of Signals in Noise*. Academic Press, 1971.

UNCLASSIFIED   -39-

SECURITY CLASSIFICATION OF FORM
(highest classification of Title, Abstract. Keywords)

DOCUMENT CONTROL DATA

(Security classification of title, body of abstract and indexing annotation must be entered when the overall document is classified)

1. ORIGINATOR (the name and address of the organization preparing the document. Organizations for whom the document was prepared, e.g. Establishment sponsoring a contractor's report, or tasking agency, are entered in section 8.) Defence Research Establishment Ottawa 3701 Carling Ave Ottawa, Ontario, Canada K1A OK2	2. SECURITY CLASSIFICATION (overall security classification of the document. including special warning terms if applicable) UNCLASSIFIED

3. TITLE (the complete document title as indicated on the title page. Its classification should be indicated by the appropriate abbreviation (S,C or U) in parentheses after the title.)

PEAK DETECTION OF SWERLING TYPE TARGETS PART I: DETECTION PROBABILITIES IN WHITE NOISE (U)

4. AUTHORS   (Last name, first name, middle initial)

Drosopoulos Anastasios, Haslam George

5. DATE OF PUBLICATION (month and year of publication of document) December 1993	6a. NO. OF PAGES (total containing information. Include Annexes, Appendices, etc.) 48	6b. NO. OF REFS (total cited in document) 10

7. DESCRIPTIVE NOTES (the category of the document, e.g. technical report, technical note or memorandum. If appropriate, enter the type of report, e.g. interim, progress, summary, annual or final. Give the inclusive dates when a specific reporting period is covered.)

DREO TECHNICAL REPORT

8. SPONSORING ACTIVITY (the name of the department project office or laboratory sponsoring the research and development. Include the address.)

Defence Research Establishment Ottawa
3701 Carling Ave.
Ottawa, Ontario, Canada K1A OZ2

9a. PROJECT OR GRANT NO. (if appropriate, the applicable research and development project or grant number under which the document was written. Please specify whether project or grant) 021LA	9b. CONTRACT NO. (if appropriate, the applicable number under which the document was written)
10a. ORIGINATOR'S DOCUMENT NUMBER (the official document number by which the document is identified by the originating activity. This number must be unique to this document.) DREO REPORT 1193	10b. OTHER DOCUMENT NOS. (Any other numbers which may be assigned this document either by the originator or by the sponsor)

11. DOCUMENT AVAILABILITY   (any limitations on further dissemination of the document, other than those imposed by security classification)

(X) Unlimited distribution
( ) Distribution limited to defence departments and defence contractors; further distribution only as approved
( ) Distribution limited to defence departments and Canadian defence contractors: further distribution only as approved
( ) Distribution limited to government departments and agencies; further distribution only as approved
( ) Distribution limited to defence departments; further distribution only as approved
( ) Other (please specify):

12. DOCUMENT ANNOUNCEMENT   (any limitation to the bibliographic announcement of this document. This will normally correspond to the Document Availability (11). However, where further distribution (beyond the audience specified in 11) is possible, a wider announcement audience may be selected.)

13. **ABSTRACT** (a brief and factual summary of the document. It may also appear elsewhere in the body of the document itself. It is highly desirable that the abstract of classified documents be unclassified. Each paragraph of the abstract shall begin with an indication of the security classification of the information in the paragraph (unless the document itself is unclassified) represented as (S), (C), or (U). It is not necessary to include here abstracts in both offical languages unless the text is bilingual).

Peak detection is an alternative to the commonly used threshold detection scheme in radar systems. The present report is the first part in an investigation of peak detection performance, for Swerling type targets, in an arbitrary noise/ clutter background. In this report, peak detection is compared with classic fixed threshold detection in uncorrelated white noise. ' ethodology is also developed, capable of handling arbitrary stochastic signal and noise/clutter models.

14. **KEYWORDS, DESCRIPTORS or IDENTIFIERS** (technically meaningful terms or short phrases that characterize a document and could be helpful in cataloguing the document. They should be selected so that no security classification is required. Identifiers, such as equipment model designation, trade name, military project code name, geographic location may also be included. If possible keywords should be selected from a published thesaurus. e.g. Thesaurus of Engineering and Scientific Terms (TEST) and that thesaurus-identified. If it is not possible to select indexing terms which are Unclassified, the classification of each should be indicated as with the title.)

Radar Detection
Peak Detection